Islamic Azad University
Mashhad Branch

Primary analysis for enhancing the iron oxide and alteration minerals, using ETM$^+$ data: a case study of Kuh-e-Zar gold deposit, NE Iran

S. Saadat[*1] and M. Ghoorchi[2]

1. Department of Geology, Faculty of Sciences, Islamic Azad University, Mashhad Branch (University of Colorado, Boulder Co.)
2. Research & Exploration Center for Ore Deposit of Eastern Iran, Ferdowsi University of Mashhad
Received 11 November 2008; accepted 25 June 2009

Abstract

Different types of iron oxides deposits have been identified along the Khaf – Dorouneh volcanic and plutonic belt in north east of Iran. Kuh-e-Zar is one of these ore deposits known as Fe- oxide gold deposit. The main purpose of this paper is to detect and discriminate the iron oxide minerals in this area based on the ETM$^+$ data. Data processing has been done by ENVI (Environment for Visualizing Images) software. Color Composites, Band Ratios, Principal Components (PC) analysis were used to delineate the associated zones of hydrothermal alteration and iron oxide minerals. Based on both field observations and the results of this satellite data processing, the area covered by secondary iron oxide (hematite, goethite and limonite mainly in soil) was enhanced very good, but the primary iron oxides (specularite) which are very fine grain and have a linear structure (mainly in mineralized veins) are not very clear in detail in these images.

Keywords: *Fe-oxide gold deposit, ETM$^+$ data, Kuh-e-Zar, Iran*

1. Introduction

Remote sensing plays an important role in the mineral exploration. One of the common applications is to locate alteration zones related to the mineral deposits. The remote sensing data can be used to map alteration zones rapidly and cheaply (Yongming et al, 2004). Different types of iron oxides deposits have been identified along the Khaf Dorouneh volcanic and plutonic belt in north-eastern Iran. Kuh-e-Zar is one of these ore deposits known as Fe- oxide gold deposit. Based on the vast improvements in geology and mineral exploration through remote-sensing techniques, we have tried to use satellite data for better understanding of distribution of iron oxide minerals in this area.

Iron oxide minerals have characteristic yellowish or reddish color to the altered rocks, but based on field observation we have identified two types of iron oxide minerals; fine-grained specularite with black color, mainly found in mineralized veins and secondary iron oxide (such as hematite or limonite) with reddish or yellowish color mainly covering the western part of the area.

The main purpose of this paper is to detect and discriminate the iron oxide minerals in this area based on the ETM$^+$ data. High quality images have been used for better understanding of the geological setting the relationship between iron oxide distribution and gold mineralization in this area and also for this type of mineralization in whole Khaf- Dorouneh volcano-plutonic belt in north-eastern Iran.

2. Geology and mineralization

The study area is located 180 km south of Mashhad (The second most populated city in Iran) and is limited between 58° 50’ - 58° 57’ east longitude, and 35° 20’ - 35° 25’ north latitude with an approximate area of about 40 km^2. The nearest populated center is the village of Fadiheh (Fig. 1). The Iranian plateau occurs within a part of the active Alpine-Himalayan orogenic belt. The Khaf- Dorouneh volcano- plutonic belt is located in north-east of this plateau with an east-west trending and around 500 Km length in north of Dorouneh fault. The area of interest is situated within the middle part of this volcano-plutonic belt. The east-west trending Dorouneh fault divides the area into the northern and southern regions (Fig. 1). To the north of this fault, Paleogene igneous rocks are widespread, whereas to the south of this fault, Oligocene and Miocene strata including clastic sediments are present (Geological Map of Faizabad, sheet 7760).

---
*Corresponding author.
E-mail address (es): Saeed.Saadat@Colorado.edu

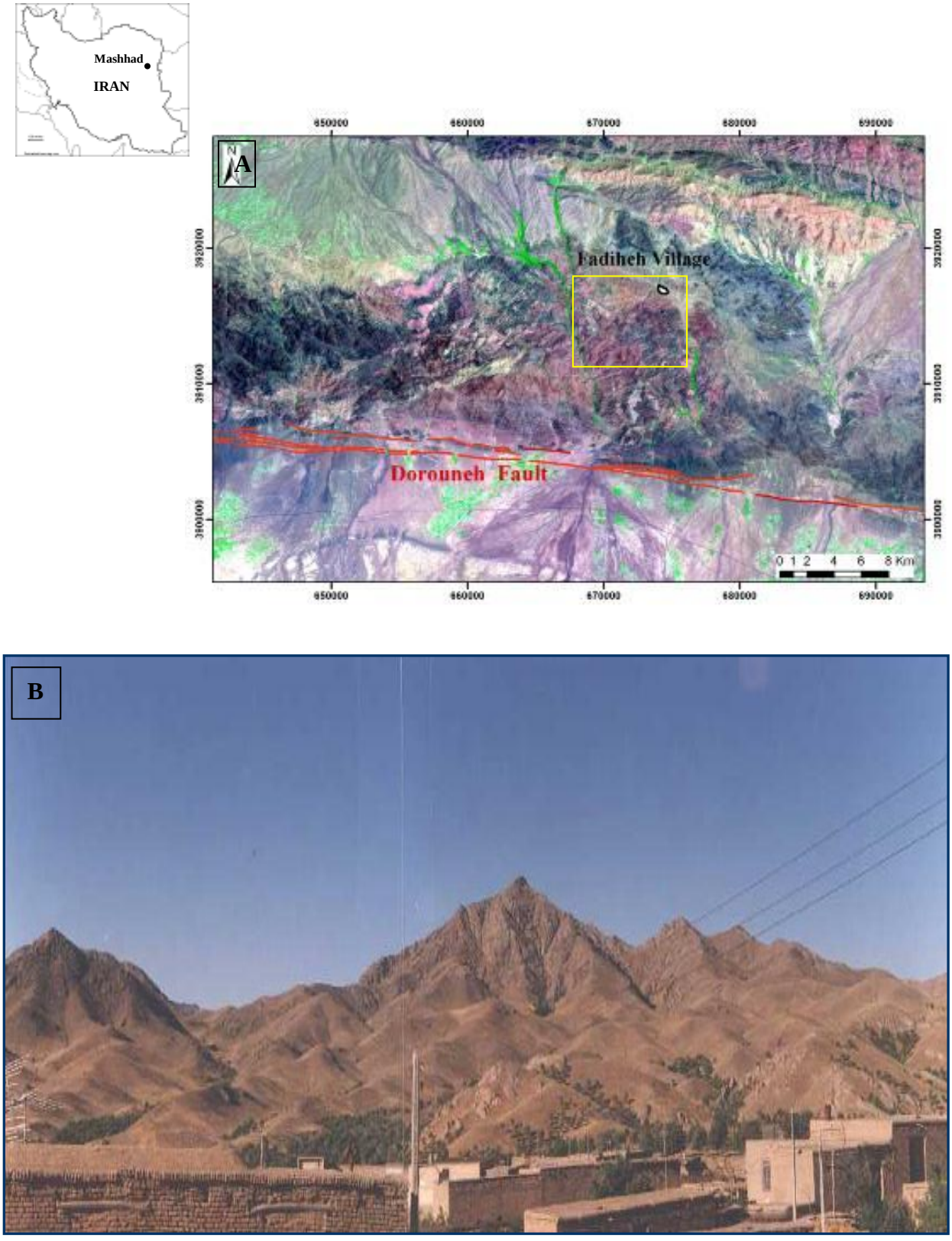

Fig. 1. A) Location of study area and Dorouneh fault in north- eastern Iran. B) village of Fadiheh which is located in the north of the study area (looking to the south).

Judging by the existence of a layer of nummulitic limestone between the volcanic rocks; magmatic activity in this area can be dated to Eocene time. Presence of limestone and some epiclastic volcanic sandstone within different parts of the volcanic sequence indicate different cycles of volcanism during Eocene (Zarmehr Gold Company, internal report, 2003). Volcanic rocks are mainly intermediate to felsic in the study area. Majority of volcanic rocks are pyroclastic type with some intercalated lava flow. Welded and lapili tuff are dominant, lava consists of andesite, latite and trachyte porphyry and hornblende latite(Fig. 2). Different types of intrusive rocks are noticed in the study area which are mainly granite and hornblende monzonite porphyry, latite porphyry and microdiorite (Fig. 2). These rocks are mainly greenish grey color. Most of them have a porphyritic texture with large phenocrysts. The macroscopic components of the studied rocks are quartz, potassium feldspar, plagioclase feldspar and amphibole. The absolute age of intrusive rocks are not known, since they intruded into volcanic rocks, therefore they are younger than Eocene. Based on the wide range of chemical composition of intrusive rocks, it seems that magmatic activity took place at different times.

Mineralization is mainly structurally controlled and localized along the faults and within the fault zones. Two sets of steep, strike-slip faults are present in the study area. One series is trending N60°E to EW and the second series is N20°W. Rocks are highly brecciated within the faults and fault zones. Gold bearing solutions filled spaces between these breccias (Zarmehr Gold Company, internal report, 2003). Fifteen mineralized faults are identified that control the geometry of mineralization associated with both stockwork and hydrothermal breccias. Paragenesis involves specularite-quartz-gold-chlorite ± chalcopyrite ± pyrite ± galena ± barite. Specularite is fine-grained and forms 20 to 60% of the veins. In a few localities, chalcopyrite and minor pyrite and galena are also found. SEM studies have revealed that gold is fine-grained (<40 micron). Propylitic alteration covers large area. Silicification is found within the fault zones.

Albite-chlorite alteration is identified within the intrusive. Argillic was formed due to sulfide oxidation. Gold grades are 0.07 – 36 ppm, Ag average 20 ppm, As and Sb < 30 ppm, Cu is < 50 ppm but in some zones up to 8000 ppm, Pb 50-3000 ppm, and Zn 70-2500 ppm (Mazlumi, et al., 2007).

3. Methods

A scene of LandSat Enhanced Thematic Mapper plus (ETM+ data, path 159, row 36, date 2000) including Kuh-e-Zar area is used for this study. This image is geometrically corrected by using control points from topographic sheets. Data processing has been done by ENVI (Environment for Visualizing Images) software. Color Composites, Band Ratios, Principal Components (PC) analysis were used to delineate the associated zones of hydrothermal alteration and iron oxide minerals. Color composite images are the most basic form of spectral analysis. The selection of specific spectral bands for display in the red, green, and blue image plains of a computer. display can be used for rapid first-order analysis of the spectral properties of a scene. Soil and rocks with abundant iron oxides exhibit low reflectance in band 3, with moderate to high reflectance in bands 4 and 7, and regions rich in these minerals exhibit the distinctive yellow colors. Ratio images created, by dividing one spectral image channel by another pixel by pixel, are widely used in earth science investigations because of the proven ability of ratio images to enhance the discrimination of the surface units (Rencz, 1999). The principal component analysis is widely used for alteration mapping in metallogenic provinces (Kaufman, 1988; Crosta and Moore, 1989; Loughlin, 1991; Benett et al, 1993 and Rutz-Armenta and Prol-Ledesma, 1998). Principal component analysis (PCA) is a data compression method, applied to compress redundant data into fewer bands; the reduction of the bands (also called components) facilitates the interpretation of data (Jensen, 1986). Applying PCA creates a new data set with fewer variables (Lillesand and Kiefer, 2000).

4. Conclusions

Based on the common multi-spectral ratios for the minerals shown in table 1, the ratios of band 3 to band 1 (TM) for materials lacking ferric compounds will be close to unity (e.g., montmorillonite and kaolinite) while for ferric-bearing compounds such as hematite and goethite this ratio will be much greater than 1 (Rencz, 1999).

Iron oxide minerals also have high reflectance in ETM^+ band3 and band 5 and high absorption in ETM^+ band 1 and band 4 (Fig. 3). We used the ratio of band3+band5/band1+band4 for enhancing the areas that is covered by iron oxide minerals. According to this technique areas with abundant iron oxides indicate bright pixels (Fig. 4).

Argillic alteration minerals (mainly clay minerals) have high reflectance in wavelength 1.55- 1.75 micrometer and high absorption with wavelength 2.35- 2.8 micrometer. These wavelengths are covered by ETM^+ band 7 and band 5 (Fig. 5).

Based on this characteristic, the Crosta technique (Crosta & More, 1989) is found to be very useful for enhancing the altered areas with hydroxyl and iron oxide minerals (Ranjbar et al., 2004). The Crosta technique is applied to six (1, 2, 3, 4, 5 and 7) and two sets of four (1, 3, 4, 5 and 1, 4, 5, 7) bands of ETM+ data (Crosta & Moore 1989; Loughline, 1991).

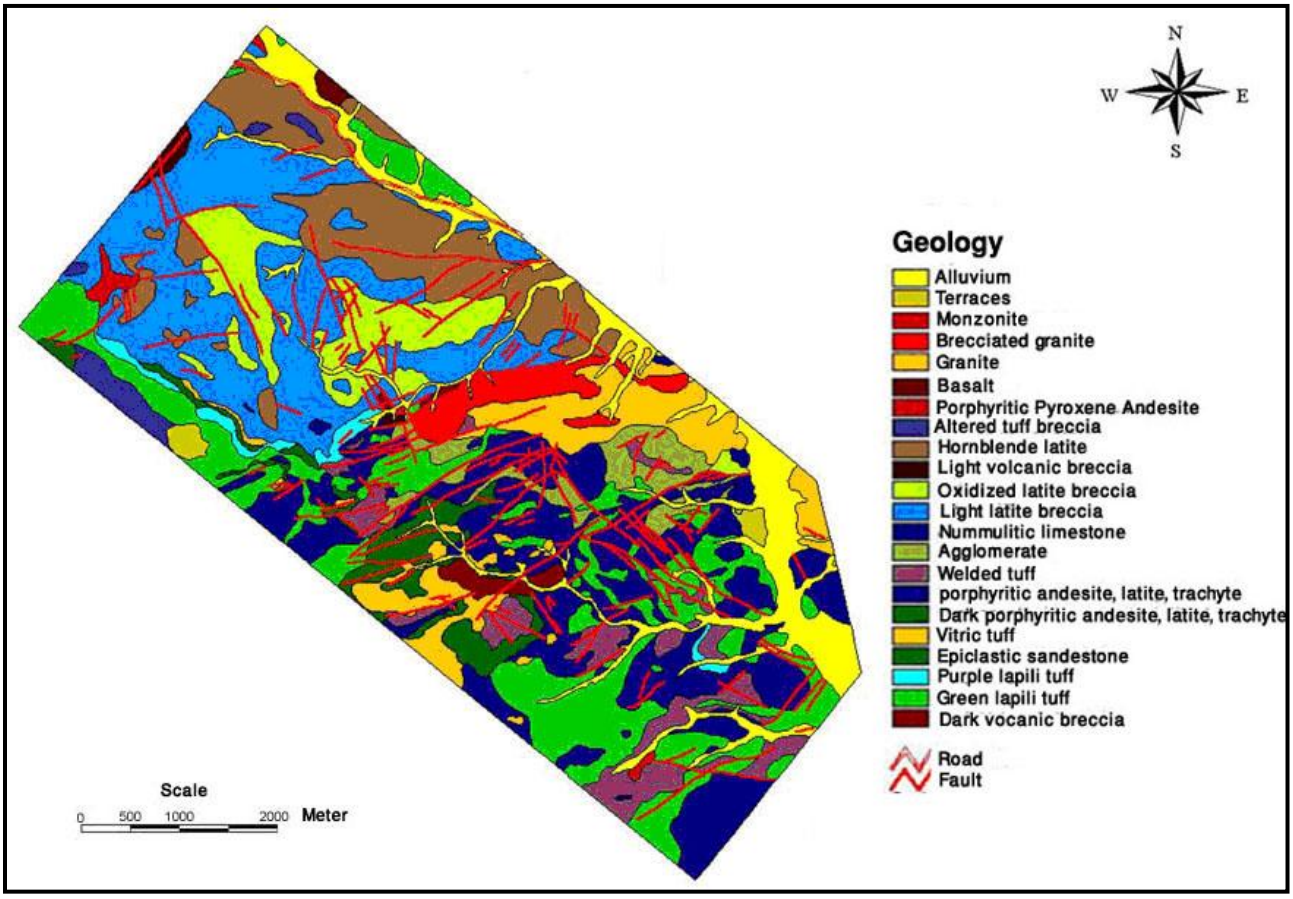

Fig 2. Geological map of Kuh-e-Zar area (Zar-Mehr Gold Company, internal report, 2003)

Table 1. TM band ratio for some minerals (Rencz, 1999)

Mineral	3/1	5/4	5/7	3/4* 5/4
Montmorillonite	1.1262	0.95793	0.61064	0.60173
Kaolinite	1.1262	1.0033	0.67157	0.65574
Hematite	7.2598	1.8767	0.07343	0.06211
Goethite	3.8719	1.9934	0.14474	0.13756

The selective PC analysis of ETM$^+$ using bands 1, 3, 4, and 5 was used in mapping iron oxide bearing minerals. The same method was also applied using bands 1, 4, 5, and 7 for hydroxyl bearing minerals detection. The eigenvector matrix generated by selecting mentioned band combination to map hydroxyl minerals and iron oxide are shown in table 2 and 3.

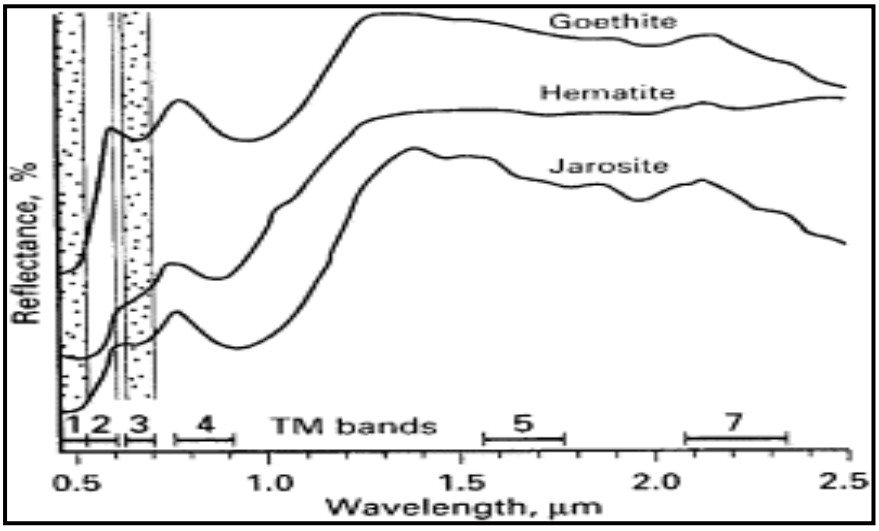

Fig. 3. Spectral reflectance curves for jarosite, hematite and goethite (after Hunt et al., 1978 and Sabins, 1997).

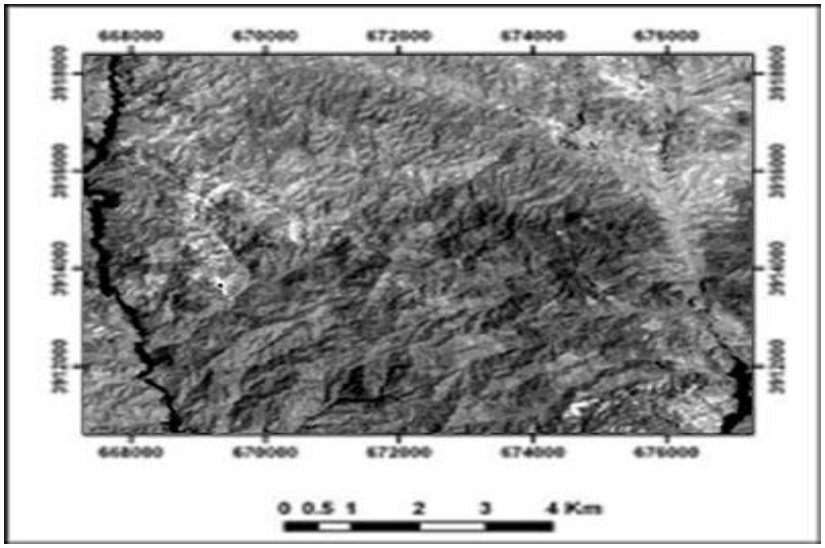

Fig. 4. The areas with abundant iron oxide minerals are shown as bright pixels.

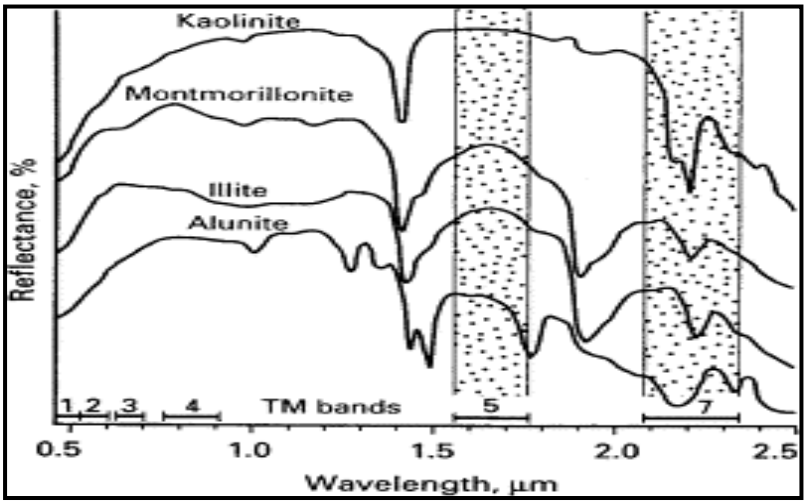

Fig. 5. Reflectance spectra of some common clay minerals (after Rowan et al., 1977 and Sabins, 1997).

Table 2. Eigenvectors of the covariance matrix of 4 band combination (TM1, TM4, TM5, TM7)

Correlation Eigen vectors	PC1	PC2	PC3	PC4
Band1	0.494028	0.592847	0.043709	0.634475
Band4	0.560458	0.329499	-0.211850	-0.729683
Band5	0.492268	-0.635717	-0.540428	0.247939
Band7	0.446650	-0.368546	0.813109	-0.059429

Table 3. Eigenvectors of the covariance matrix of 4 band combination (TM1, TM3, TM4, TM5)

Correlation Eigenvectors	PC1	PC2	PC3	PC4
Band1	0.528165	-0.176692	0.677975	0.479762
Band3	0.464687	-0.738604	-0.475448	-0.111712
Band4	0.571940	0.367041	0.157166	-0.716564
Band5	0.421891	0.537146	-0.538143	0.493847

Table 2 and 3, PC1 give information mainly on albedo and topography (Ranjbar et al., 2004). In PC3 vegetation and in PC4 the hydroxyl minerals are enhanced. In table 2, according to the negative value for band 7 (max. absorption for hydroxyl minerals) and positive value for band 5 (max. reflectance for hydroxyl minerals), PC4 is very useful for enhancing the altered areas with hydroxyl minerals. In order to map iron oxide, input bands are restricted to TM1, TM3, TM4 and TM5. Eigenvector values of the table 3 show that PC3 maps the iron oxide. In PC3, according to the negative value for band3 (max. reflectance for iron oxide minerals) and positive value for band 1 (max. absorption for iron oxide minerals), the Fe oxide are highlighted as dark pixels so this image must be negated to map Fe oxide as bright pixels (Fig. 6). Final color composite (RGB) was made by using the inverse PC3(1, 3, 4, 5), PC4(1, 4, 5, 7), and TM4 is shown in figure 7. The resultant is good enough for demarcating iron oxide minerals. Principal component analysis (table 4) was done using six ETM^+ bands as input bands (bands 1, 2, 3, 4, 5 and 7). The first principal component does not contain spectral features relevant in this analysis, as it is a combination of all the Bands. This PC gives information mainly on albedo and topography (Ranjbar et al., 2004). Vegetation is enhanced in PC4 and hydroxyl minerals are enhanced in PC6. Hydroxyl image that is prepared by using eigenvector loadings of PC6 is shown in Figure 8. A similar analysis of PC3 shows that the most important contributions come from TM1 and TM3 but with opposite signs. According to spectral characteristics of iron oxide (Hunt et al., 1978), it will be mapped by dark pixels.

Based on Loughlin's technique (1991), a false color composite image is made (PC4 in Red, PC4+PC5 in green and PC5 in blue). In the resulted image hydroxyl minerals are shown in red, iron oxide in blue and sum of these two are shown in bright pixels (Fig. 9).

According to Bushara (1996) a false color composite image is made by PC4, PC5, PC6 in RGB, the alteration area is shown in dark red (Fig. 10).

5. Results

In this study we tried to use Landsat ETM^+ data to delineate the areas of iron oxides and hydrous minerals in one of iron oxide- gold deposits. Based on both field observations and the results of this satellite data processing, the area covered by secondary iron oxide (hematite, goethite and limonite mainly in soil) was enhanced very nicely, but the primary iron oxides (specularite), which are very fine-grained and have a linear structure (mainly in mineralized veins), are not very clear in detail in these images.

Morris et al. (1985) studied the details of submicron size iron oxides, where it was found that the absorption bands decrease rapidly in intensity. This occurs because the increased surface/volume ratio at small grain size results in a greater proportion of grain boundaries where crystal field effects are different, resulting in lower magnetic coupling and reduced absorption strength. Other iron oxides probably show similar effects. Reflectance spectra of iron oxides have such strong absorption bands that the shape changes significantly with grain size.

Although during the recent years, remote sensing techniques have developed strongly but it seems that distinguishing with reflectance spectroscopy for various types of iron oxide minerals is still a matter of research.

Table 4. Eigenvector and percentage of variance of the principal components for six bands of ETM^+

	PC1	PC2	PC3	PC4	PC5	PC6
Band1	0.50	0.49	0.20	-0.48	0.49	0.01
Band2	0.56	0.46	-0.22	0.43	-0.50	-0.03
Band3	0.31	-0.38	-0.82	-0.26	0.14	-0.04
Band4	0.48	-0.49	0.32	0.50	0.37	-0.18
Band5	0.29	-0.32	0.24	-0.24	-0.32	0.77
Band7	0.19	-0.25	0.28	-0.46	-0.49	-0.61
Variance %	84.34	8.27	5.73	0.84	0.65	0.17

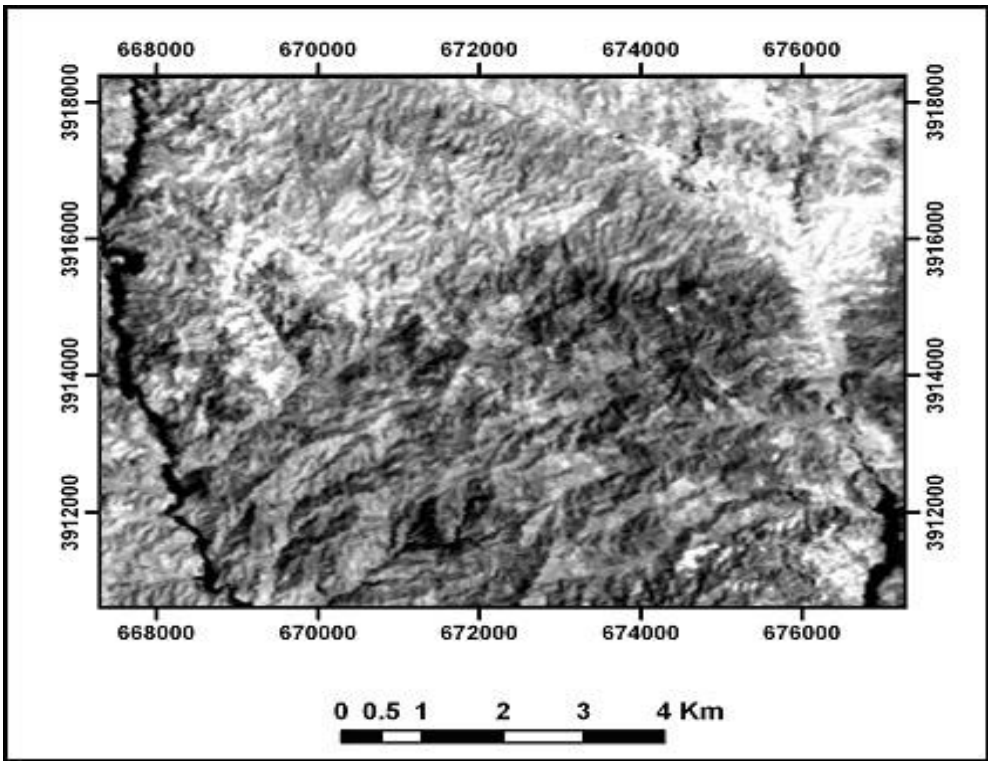

Fig. 6. Image obtained by using the eigenvector loadings of PC3 (1, 3, 4, 5) for enhancing iron oxide. Iron oxide minerals are shown as bright pixels in study area.

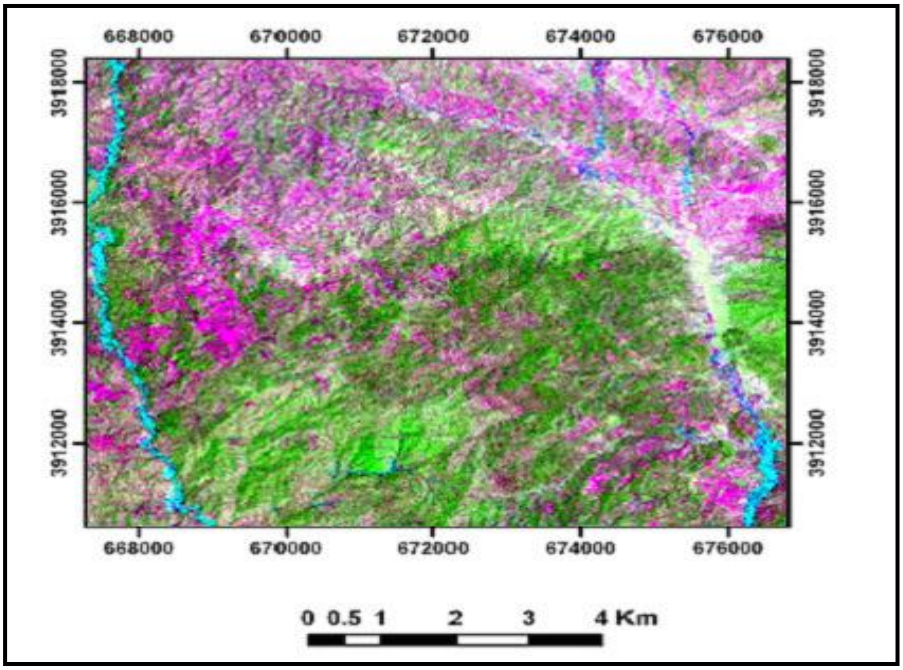

Fig. 7. RGB color composite image of inverse PC3 (1, 3, 4, 5), PC4 (1, 4, 5, 7), and TM4. See text for explanation.

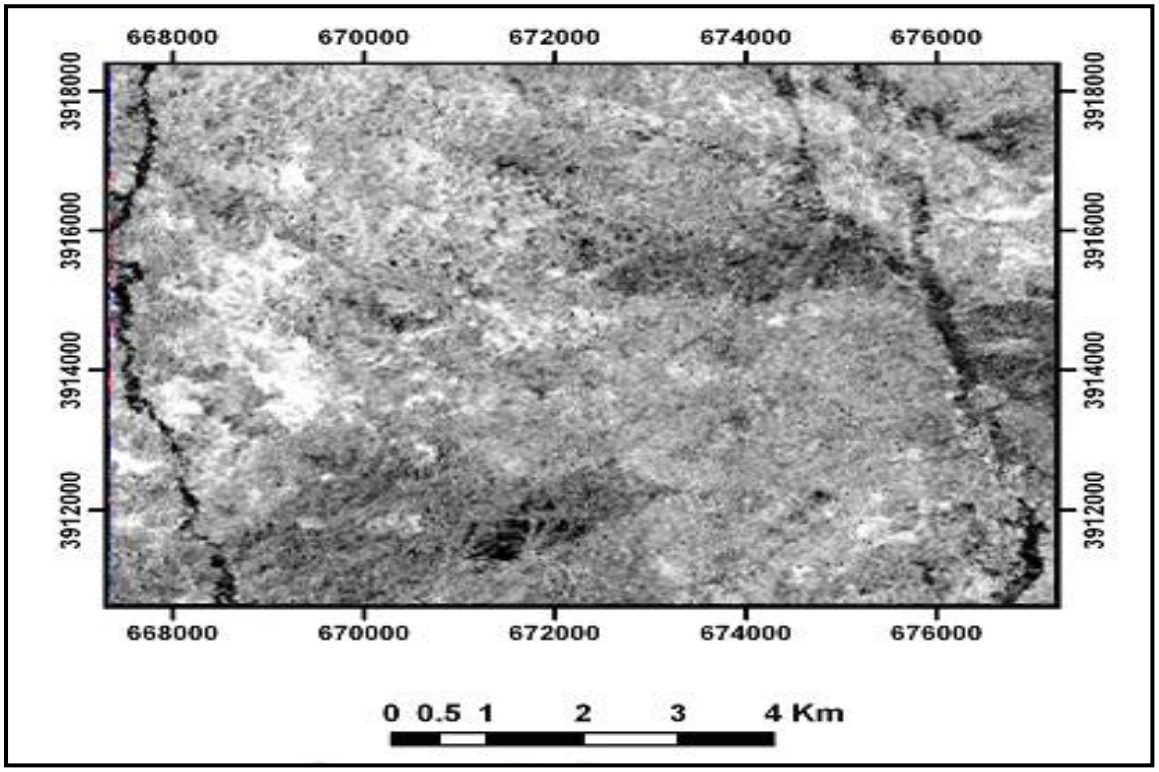

Fig. 8. This image is obtained by using the eigenvector loadings of PC6 for enhancing Hydroxyl minerals. The bright pixels are the areas with Hydroxyl minerals.

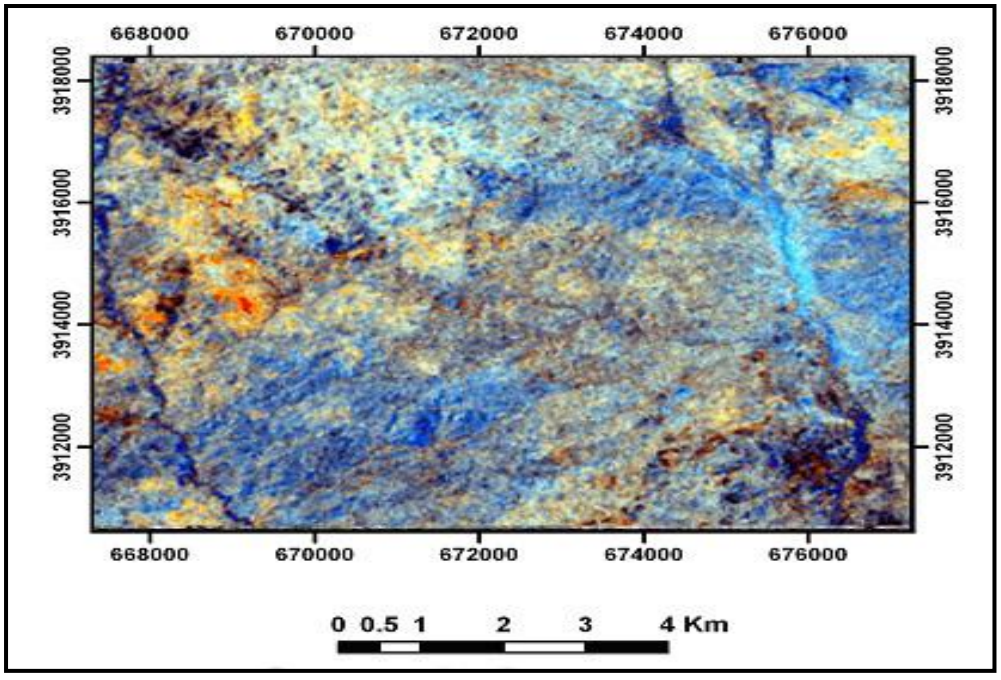

Fig. 9. This image is obtained by making RGB of PC4 (red), PC5 (blue) and PC4+PC5 (green). Iron oxide minerals are shown as blue pixels. Hydroxyl minerals are shown in red. Bright pixels are both hydroxyl and iron oxide minerals.

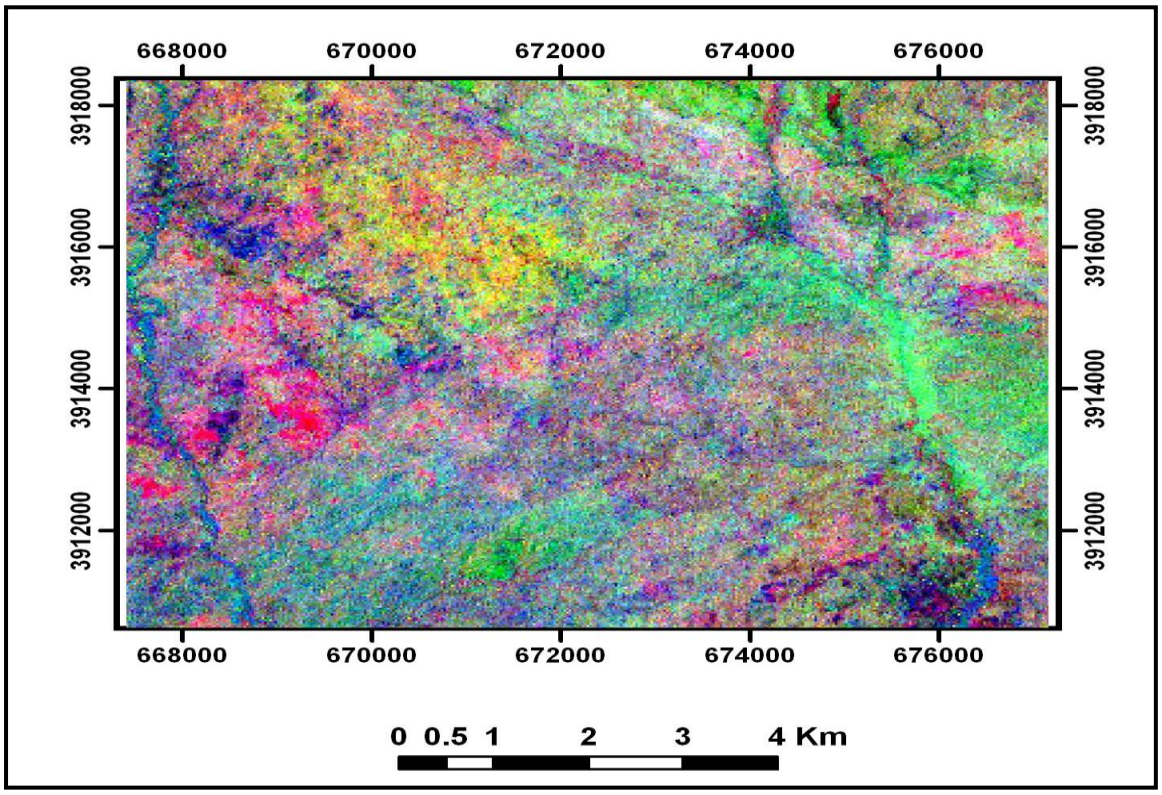

Fig. 10. This image is obtained by making RGB of PC4 in red, PC5 in green and PC6 in blue.

Acknowledgments

The authors are indebted to Dr. Khalid Hussein for his suggestions, advice and review of an earlier version of this manuscript and to Professor M. H. Karimpour for his very useful suggestions and for providing ETM^+ data including Kuh-e-Zar area. The authors are also grateful to the professor M. Pandit for his constructive comments as a reviewer of the Iranian Journal of Earth Sciences.

References

Bennet, S. A., Atkinson, W.W, Kruse, F. A., 1993. Use of Thematic Mapper imagery to identify mineralization in the Santa Teresa district, Sonara, Mexico. International Geology Review, pp. 1009-1029.

Bushara, M.N., 1996. Neogene geologic structures using enhanced Thematic Mapper over eastern Zagros Mountains. Int. J. Remote Sensing, 172, pp. 303–313

Crosta, A. and Moore, J. McM., 1989. Enhancement of Landsat Thematic Mapper imagery for residual soil mapping in SW Minais Gerais State, Brazil: a prospecting case history in Greenstone belt terrain. In: Proceedings of the 7th ERIM Thematic Conference: Remote sensing for exploration geology, pp. 1173-1187.

Floyd F. Sabins, 1998. Remote sensing for mineral exploration The Leading Edge; v. 17; no. 4; p. 467-470.

Geological Survey of Iran, 1987. Geological map of Iran, 1:100000 Series, sheet 7760, Faizabad.

Hunt, G. R., Salisbury, J. W., and Lenhoff, G. J., 1978. Visible and near-infrared spectra of minerals and rocks: III Oxides and hydroxides, Modern Geology, 2: 195-205.

Jensen, J. R., (Ed.), 1986, Introductory Digital Image Processing, Englewood Cliffs, New Jersey: Prentice-Hall. Pp. 368.

Kaufman, H., 1988. Mineral exploration along the Agaba-Levant structure by use of TM-data concepts, processing and results. International Journal of Remote Sensing, 9: 1630-1658

Lillesand, T.M. and Kiefer, R.W., (Ed.), 2000, Remote Sensing and Image Interpretation, New York, John Wiley & Sons. 724 pages

Loughlin, W. P., 1991. Principal Component Analysis for alteration mapping. Photogrammetric Engineering and Remote Sensing, 57: 1163-1169.

Mazloumi, A.R., Karimpour, M. H., Stern, Ch. R., Rassa, I., and Saadat, S., 2007. Fluid inclusion thermometry, S-isotop, petrology of Kuh-e-Zar specularite rich iron oxide gold deposit, north eastern. GSA Annual Meeting, Denver, Colorado.

Morris,R. V., H. V. Lauer, C. A. Lawson, E. K. Gibson, Jr., G. A. Nace, and C. Strewart, 1985. Spectral and other physiochemical properties of submicron powders of hematite, maghemite, goethite, and lepidochrosite, J. geophys. Res., 90, 3126-3144.

Ranjbar H, Honarmand M, Moezifar Z, 2004. Application of the Crosta technique for porphyry copper alteration

mapping, using ETM+ data in the southern part of the Iranian volcanic sedimentary belt. Journal of Asian Earth Science, volume: 24 Issue: 2 Pages: 237-243

Rencz, A. N. 1999, Remote sensing for the Earth Sciences, 3ed., Vol. 3. John Wiley & Sons, Inc. 707 p.

Rowan, L.C., Goetz, A.F.H. and Ashley, R.P., 1977. Discrimination of hydrothermally altered and unaltered rocks in visible and near infrared multispectral images. Geophysics 42, pp. 522–535.

Sabins, F.F., 1997. Remote Sensing, Principles and Interpretation. (third ed.), Freeman, New York 494 pp

Rutz-Armenta, J. R. and Prol-Ledesma, R. M., 1998. Techniques for enhancing the spectral response of hydrothermal alteration minerals in Thematic Mapper images of Central Mexico, International Journal of Remote Sensing, 19: 1981-2000.

Xu, Y., Lin, Q., Shao, Y., Wang , Lu., 2004. Extraction mechanism of alteration zones using ASTER imagery, Geoscience and Remote Sensing Symposium, 2004. IGARSS '04. Proceedings. IEEE International.

Zar mehr Gold Company, Iran, internal report, 2003.